Optimum Lift-Drag Ratio for a Ram Wing Tube Vehicle

TIMOTHY M. BARROWS*

AND

SHEILA E. WIDNALL†
Massachusetts Institute of Technology, Cambridge, Mass.

Munk's theorem specifying the downwash condition for minimum drag is generalized to include lifting surfaces operating in proximity to solid boundaries. A simple method for finding the optimum lift distribution on a wing above an infinite flat plane is developed. The optimum configuration for a ram wing in a tube is found, and by means of a simple transformation this is mapped into the previously obtained solution for a wing in ground effect. An expression for the induced power required is calculated, and it is shown that there is a favorable effect on this requirement for the case of tube vehicles which have significant blockage ratios. Experimental results are presented which demonstrate that at very small clearances the theory must be modified to include viscous effects, and because of these effects ram wings in tubes usually have lower induced power requirements than the inviscid theory would indicate.

Nomenclature

AR = aspect ratio
A_t = cross-sectional area of tube
b = wing span = vehicle width
C_{D_i} = induced drag coefficient
C_L = lift coefficient
D_i = induced drag
F = volume flux
G = gap
K = aspect ratio augmentation factor (see Fig. 10)
KE = kinetic energy
L = lift
P = power required for lift
r = blockage ratio = A_v/A_t
s = spanwise position coordinate (see Fig. 3)
S = contour enclosing the trailing vortices (see Fig. 2)
U = x velocity past vehicle
U_∞ = x velocity far downstream of vehicle. If the fluid far downstream is stationary, U_∞ = vehicle velocity relative to tube
v_l = tangential velocity under the wing
v_n = velocity normal to the vortex wake
v_t = velocity tangential to the vortex wake
w_o = downwash at the center of the vortex wake
x = axial coordinate
X = $y + iz$
y = lateral coordinate
z = vertical coordinate
α = angle of attack
β = angle of inclination (see Fig. 3)
γ = trailing vortex strength
Γ = bound vortex strength
δ = variational quantity
Δ = small increment
ϵ = clearance ratio (see Fig. 5)
ζ = transformed vertical coordinate
η = transformed lateral coordinate
θ = (see Fig. 4) integration angle
λ = Lagrange multiplier
ξ = $\eta + i\zeta$
ρ = air density
Σ = (see Fig. 2) outer contour of integration
ϕ = nondimensional velocity potential
ψ = nondimensional stream function
∇ = gradient

Subscripts

i = induced
l = lower surface of wing
n = normal
t = tangential
v = vehicle
$*$ = dimensional quantity
X = quantity in X plane
ξ = quantity in ξ plane

Received December 27, 1968; revision received August 29, 1969.

* Graduate Student, Department of Mechanical Engineering.
† Assistant Professor, Department of Aeronautics and Astronautics. Member AIAA.

Introduction

IN recent years a great deal of interest has been generated concerning the concept of using a tube as a guideway for high-speed ground transportation vehicles. The need here is to develop a safe and reliable intercity system that can deliver passengers from city center to city center at speeds in the range of 200 to 400 mph. As higher and higher speeds are contemplated, it becomes increasingly attractive to have an enclosed vehicle guideway; a tube of circular cross section fulfills this condition and, in addition, offers a number of unique advantages. Among these are: the greatest possible area for a given peripheral length, an ideal shape for withstanding the hydrostatic forces associated with being buried underground, and the ability to allow the vehicle to bank like a toboggan through turns.

A most important feature of a vehicle is the method of support. One very promising approach is to use a ram wing; that is, the vehicle can utilize aerodynamic forces and support itself with forward speed effects. "Ram wing" is a general term which stands for any lifting surface operating in proximity to the ground or some other solid boundary.

The presence of a guideway around a lifting surface offers a number of intriguing possibilities. Not the least of these is the fact that, since the domain in which the wing operates is bounded, the theoretical possibility exists of operating a wing with no induced drag, so that the lift could be obtained with no power expenditure. This could be done by having a mechanical seal between the tip of the wing and the guideway, although this immediately eliminates the primary advantage of aerodynamic support—no mechanical contact

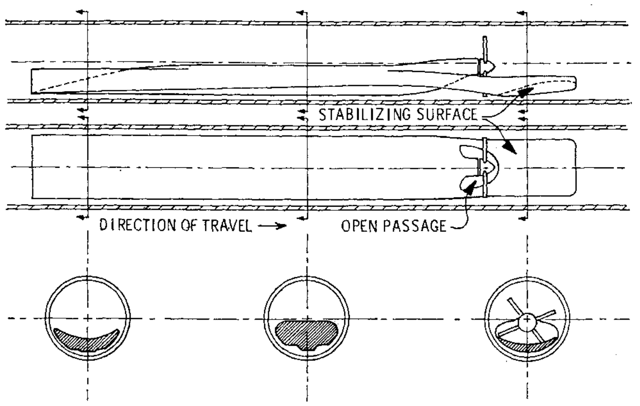

Fig. 1 Powered vehicle model developed at Princeton.

with the guideway. A second method would be to have a thin jet curtain at the wing tips which would provide a seal for the high pressure under the wing. This concept would, of course, require some power for the jet; it is discussed in Ref. 1.

All such methods for actually eliminating the induced drag involve some disadvantage, however, so that as an alternative one can instead focus on the problem of optimizing the lift-drag ratio. As can be seen in this article, very efficient wings can indeed be obtained in a tubular guideway; so efficient, in fact, that the induced drag is really negligible compared with the parasite drag. In addition, the solution of the minimum drag problem gives a great deal of insight into the nature of the flowfield of a ram wing.

As an illustration of the ram-wing-in-tube concept we have in Fig. 1 a sketch of a vehicle model which has been the subject of some experimental study.‡ In this case the entire vehicle is a ram wing with a small stabilizing surface in the front, and a propeller for propulsion. The model itself was 6 ft long and flew in a 1 ft diam tube at speeds approaching 50 mph using a model airplane engine. The minimum clearance of the model at its maximum speed was one inch; it was inherently stable and required no special devices to prevent it from drifting into the side of the tube. Further information in this model may be found in Ref. 2.

Presently the possibilities of ram wing support for tube vehicles are being investigated at Rensselaer Polytechnic Institute. They have formulated an integral equation for the two-dimensional chordwise lift distribution[3] and are currently running two-dimensional tests in a wind tunnel using a moving ground board. In addition they are correlating these results with three-dimensional tests of a ram wing in a tube.

The general problem of minimizing induced drag for arbitrary lifting surfaces operating in a freestream has been investigated by Munk.[4] Using the calculus of variations he obtained general theorems for three-dimensional lifting surfaces; these were studied in some detail more recently by Cone.[5,6] The problem of a flat wing of high aspect ratio in the center of a circular wind tunnel was studied simultaneously by Glauert[7] and Millikan.[8] In the present extension the downwash condition for minimum induced drag for a ram wing is shown to be identical with the result obtained by Munk, and a method is developed for finding the lift distribution which satisfies this downwash condition. The minimum power required for lift is calculated, and experimental results are presented which suggest that in some cases viscous effects can be quite important.

‡ This model was developed by T. Barrows, working with a colleague, T. Balsa, under the direction of M. P. Knowlton of Princeton University.

General Theory of Minimum Induced Drag

The induced drag of any lifting system may be computed by evaluating the kinetic energy of the fluid in the wake;

$$KE = \tfrac{1}{2}\rho U_\infty{}^2 \iiint_V (\nabla\phi)^2 dV \tag{1}$$

Far downstream from the wing the flow is essentially a two-dimensional trailing vortex system and Eq. (1) can be rewritten as an area integral over the tube cross section representing the kintic energy per unit length in the x direction. This energy is produced by the induced drag, and the two must be equal

$$D_i = \tfrac{1}{2}\rho U_\infty{}^2 \iint_{A_t} (\nabla\phi)^2 dA \tag{2}$$

This can be converted to a contour integral using Green's theorem

$$D_i = (\rho U_\infty{}^2/2)\int_{S+\Sigma} \phi(\partial\phi/\partial n)dS$$

S and Σ are defined in Fig. 2. The integration over Σ is zero since $\partial\phi/\partial n$ is zero on the tube surface. The integration over S becomes a line integral by noting that the discontinuity in potential across the wake is the same as the bound circulation.[9] That is,

$$\phi_{\text{upper}} - \phi_{\text{lower}} = \Gamma/U_\infty \tag{3}$$

and

$$D_i = \rho U_\infty/2\int \Gamma(\partial\phi/\partial n)ds \tag{4}$$

Here s is a spanwise position coordinate.

This result is quite general and applies to the Trefftz plane flow for any lifting surface operating near any solid boundary. For the important case in which the y and z perturbation velocities are small, the trailing vortices stream straight back from the trailing edge of the wing, so that the strength of the trailing vortex system is a function of y but not a function of x for all points behind the wing. Referring now to Fig. 3, for any position s, the vortex strength in this figure may represent that in either the Trefftz plane or a plane directly behind the trailing edge. This latter plane may be used to calculate the lift, even though the flow directly behind the wing is three-dimensional and not suitable for Eq. (4).

The lift is computed from an integration of the pressure distribution over the wing surface

$$\begin{aligned} L &= \iint \Delta p \cos\beta dxds \\ &= \rho\iint \gamma_1(x,s)U(x,s) \cos\beta dxds \end{aligned}$$

where γ_1 is the local bound vorticity on the wing. Introducing the further assumption that U is everywhere $\simeq U_\infty$, so that the flow is fully linearized, we obtain: $L = \rho U_\infty \iint \gamma_1(x, s) \cos\beta dxds$.

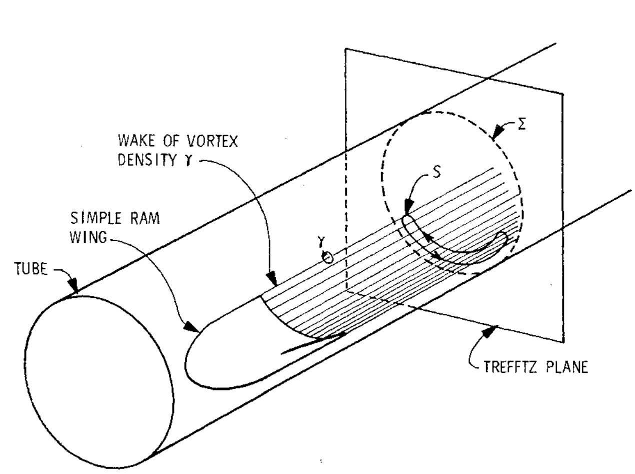

Fig. 2 Trailing vortices for the ram wing in a tube.

The spanwise circulation Γ is simply an integration over the chord

$$\Gamma(s) = \int_{L.E.}^{T.E.} \gamma_1(x,s)dx$$

This allows us to write the lift in the following form:

$$L = \rho U_\infty \int \Gamma(s) \cos\beta ds \tag{5}$$

The integration in Eq. (5) takes place in the plane directly behind the wing, but because of the preceding considerations, in the linearized case we may integrate over the same contour as Eq. (4).

It is important to note that no restrictions have been introduced on the aspect ratio of the lifting surface. It is desired to find that distribution of circulation which gives the minimum induced drag for a given amount of lift. The technique used here follows that in Ref. 10; we apply the calculus of variations to make D_i a minimum with L constrained to be constant. The proper method is to use the Lagrange multiplier λ

$$\delta D_i - \lambda \delta L = 0$$

From Eq. (2) we have

$$\delta D_i = \rho U_\infty^2 \iint_{A_t} \nabla\phi\nabla\delta\phi dA$$

Applying Green's theorem and Eq. (3) as before we obtain

$$\delta D_i = \rho U_\infty \delta \int \Gamma \frac{\partial\phi}{\partial n} ds$$

Using Eq. (5) we have

$$\delta L = \rho U_\infty \int \delta\Gamma \cos\beta ds$$

Therefore,

$$\delta D_i - \lambda\delta L = \rho U_\infty \int \delta\Gamma(\partial\phi/\partial n - \lambda \cos\beta)ds = 0$$

The only way to satisfy this for any arbitrary variation $\delta\Gamma$ is to have $\partial\phi/\partial n = \lambda \cos\beta$. It is clear that λ represents the normalized downwash at the center of the wake; i.e.,

$$\partial\phi/\partial n = (wo/U_\infty) \cos\beta \tag{6}$$

If we multiply Eq. (6) by U_∞ we obtain Munk's second theorem. This is expressed in the variables of Fig. 3;

$$v_n = w_0 \cos\beta \tag{7}$$

Munk stated his theorem in the following fashion: When all the elements of a three-dimensional lifting system have been translated into a single plane, the induced drag will be a minimum when the component of induced velocity normal to the lifting element at each point is proportional to the cosine of the angle of inclination of the element at that point.

It is interesting to note that even though Munk derived his theorem for a wing in a freestream, and specified an explicit relation between Γ and $\partial\phi/\partial n$, in fact it is not necessary to assume any relation between these variables. All that is required is that ϕ satisfy Laplace's equation and either ϕ or $\partial\phi/\partial n$ be zero on all the external boundaries. Equation (6) may be applied either in the plane of the wing or, as in this discussion, in the Trefftz plane.

We now use Eq. (4) to compute the drag increment ΔD_i from the small lifting element Δs (see Fig. 3). $\Delta D_i = (\rho U_\infty/2)\Gamma(\partial\phi/\partial n)\Delta s$. At this point we will specify that the wing has the optimum lift distribution so Eq. (6) holds, and we obtain $\Delta D_i = \frac{1}{2}\rho\Gamma w_o \cos\beta\Delta s$. We also have $\Delta L = \rho U_\infty \Gamma \cos\beta\Delta s$ and taking the ratio

$$\Delta D_i/\Delta L = D_i/L = w_0/2U_\infty \tag{8}$$

We now rewrite Eq. (5), letting $dy = \cos\beta ds$ and normalizing all lengths by dividing by the semispan. Note that with this convention $L = (\text{lift})/(\text{semispan})^2$;

$$L = \rho U_\infty \int_{-1}^{+1} \Gamma(y)dt$$

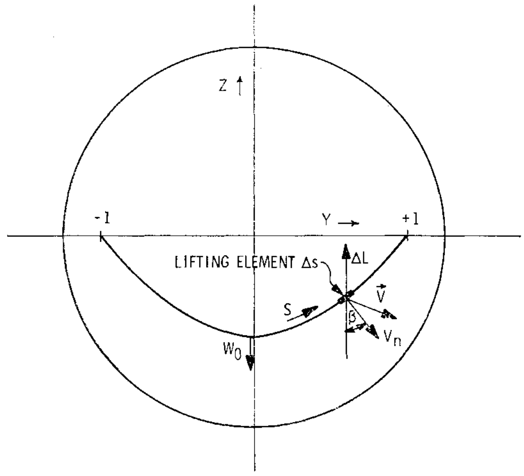

Fig. 3 Nonplanar lifting surface within enclosed guideway.

This is used to rearrange (8)

$$D_i = w_0 L^2/2\rho U_\infty^2 \int \Gamma(y)dy$$

Finally, we nondimensionalize this according to standard aeronautical notation, giving the final result

$$C_{D_i} = C_L^2/\pi K\ AR \tag{9}$$

where

$$K \equiv \frac{1}{\pi w_0} \int_{-1}^{1} \Gamma(y)dy \tag{10}$$

A similar formula was developed by Cone.[5] For a planar wing in a freestream, the theoretical optimum for K is one. The quantity $K\ AR$ is called the effective aspect ratio and it is an excellent measure of the efficiency of the lifting system.

In order to use Eq. (10) it is, of course, necessary to determine Γ. This is done by considering the trailing vortex strength γ. The two are related by $d\Gamma/ds = \gamma$.

Ram Wing in Ground Effect

Up to this point the analysis has been very general; the results apply to any lifting system and any solid boundary. Before turning to the question of ram wings in tubes, it is very useful to analyze the simpler case of a ram wing above an infinite flat plane. This problem has been solved exactly by deHaller[11] using analysis in the complex plane with multiple conformal mappings. His solution appears in terms of an infinite series of elliptic functions. Needless to say, working with this solution is somewhat awkward, and using additional transformations to extend the problem to tubes becomes extremely difficult.

A numerical procedure for predicting lift distributions on a wing in ground effect has been given by Wieselsberger,[12] and some experimental results are given in Refs. 13–15.

It is probably valid to assume that any ground transportation vehicle would operate over a fairly smooth guideway, and thus be able to have a very small vertical clearance ϵ. This allows us to obtain an extremely simple and illuminating result, as follows.

To represent the ground in the Trefftz plane we merely supply an image wing of equal and opposite vortex strength below the ground plane to make the flow symmetric about the line $z = 0$, as in Fig. 4. The simplification is based on showing that for small ϵ the tangential velocity v_t just above the wing is zero.

Consider v_t at the arbitrary point P of Fig. 4, located a small distance above the wing. In this figure θ is an obtuse angle which is chosen large enough to include all the signifi-

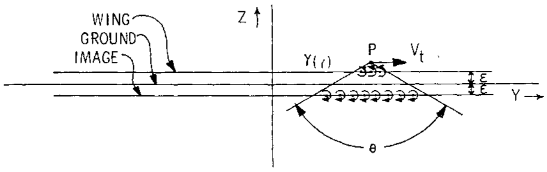

Fig. 4 Trailing vortex system for a wing at small clearance above ground.

cant vortices on the wing and image. Any vortex lying outside this angle makes a contribution to v_t which is deemed negligible. If ϵ is sufficiently small, within the angle θ the vortex strength is essentially constant. That is, the fluid at P feels the effect of two sheets of equal and opposite constant vorticity, which make equal and opposite contributions to v_t, with the net result being zero tangential velocity just above the wing. This applies all along the wing except for those points within a distance of order ϵ from the tips. Figure 4 can be redrawn to show the simple flow pattern of Fig. 5.

To a very good approximation, we have one-dimensional channel flow with mass addition in the region between the wing and the ground; that is, under the wing $v_l = w_0 y/\epsilon$.

Now γ is the same as the velocity discontinuity above and below the wing. Since $v = 0$ above the wing, $\gamma = -v_l = -w_0 y/\epsilon$. This is integrated to give the lift distribution, using the tip condition $\Gamma(1) = \Gamma(-1) = 0$;

$$\Gamma = (w_0/2\epsilon)(1 - y^2) \tag{11}$$

Thus we have the very simple result that, whereas the lift distribution on a wing in a freestream should be elliptic, as the wing comes infinitesimally close to the ground, the distribution should be parabolic. This result is in agreement with the exact solution given by de Haller.

It is a simple matter to compute K using Eqs. (10) and (11); we obtain

$$K = 2/3\pi\epsilon \tag{12}$$

Optimum Solution for a Lifting Surface in a Tube

We are now somewhat better prepared to analyze the problem of a ram wing in a tubular guideway. First, however, it is necessary to look at the engineering constraints imposed on the system and to ascertain the best configuration for the vehicle. There will be a certain minimum clearance required, which will reduce the possible area in which we can place the lifting elements of the system. This is shown in Fig. 6. All the lifting elements must fall inside the dotted lines.

It can be shown by the use of reverse flow theorems[9] that without the tube the optimum configuration is to place all the lifting elements in the outermost limit of the available area, i.e., on the dotted line of Fig. 6. The presence of the tube does not alter this result in the slightest, so that it can be immediately concluded that the best lifting surface would be a ring wing in a position concentric with the tube.

However, this is impractical for a situation as shown in Fig. 1, where the body of the vehicle is the lifting surface. Furthermore an optimally loaded ring wing has no height

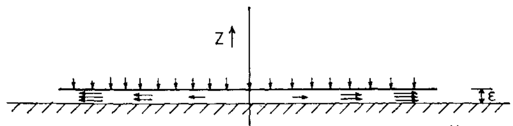

Fig. 5 One-dimensional flow under the wing trailing vortex system.

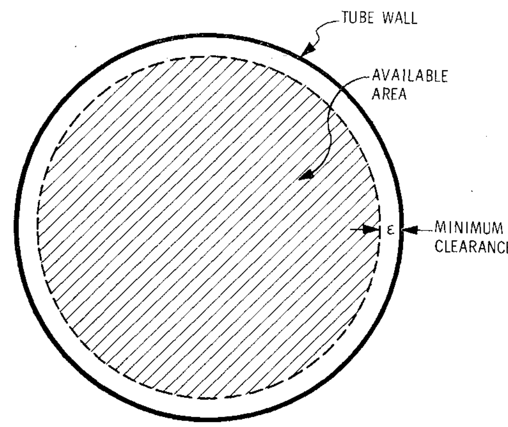

Fig. 6 Available area in Trefftz plane for lifting elements.

stability. What is desired is a single-valued contour (as opposed to a closed curve) which gives the least induced drag. The results of the previous section suggest that all of the lifting elements should be as close as possible to whatever solid boundaries are present, indicating that the best single-valued contour is a semicircle, i.e., one half of the previous circle. This suggestion is reinforced by the results given by Cone.[5] We thus arrive at the conclusion that from a practical engineering stand-point the optimum configuration is a semicircle in a concentric position.

For the sake of a more simplified analysis, and to gain maximum physical insight, it was decided to analyze a configuration which resembles the optimum case very closely, but is not quite identical. This is shown in Fig. 7; it is a semicircle which is not quite concentric with the tube. It can be seen that if the vehicle clearance ϵ is to be very small, the difference between this and the optimum is negligible.

We now map this on to the ξ plane with the following transformation: $\xi = 1/X$. It is revealed that in the ξ plane (Fig. 8) we have the equivalent of a simple wing in ground effect, and our previous results can be applied.

There is a difficult problem at this stage in properly transforming the boundary conditions. To do this we make use of the stream function ψ. Letting s represent an arc length variable as in Fig. 3, we can write

$$d\psi = (\partial\psi/\partial s)ds \tag{13}$$

To describe small changes in positions along the wing in the two planes, let $ds = d\beta$ in the X plane (Fig. 7), and $ds = d\eta$ in the ξ plane (Fig. 8).

From the properties of ϕ and ψ we have, in either plane, $\partial\psi/\partial s = \partial\phi/\partial n$. We can substitute this into Eq. (13) and

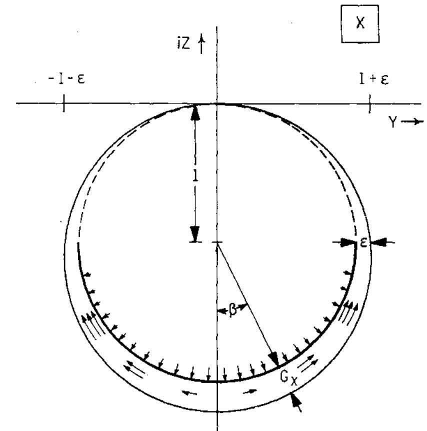

Fig. 7 Wing which closely resembles the optimum practical configuration. X plane.

take advantage of the fact that $d\psi$ must be the same in both planes, as long as we move between conformal points

$$d\psi = (\partial\phi/\partial n)_X d\beta = (\partial\phi/\partial n)_\xi d\eta \quad (14)$$

In order to be sure that we have corresponding position in both planes it is necessary to write an explicit relation between β and η; it turns out to be most convenient to express all the variables of both planes as a function of β. We have from Fig. 7

$$y = \sin\beta$$
$$z = -1 - \cos\beta$$
$$\eta = Re\left(\frac{1}{X}\right) = \frac{y}{y^2 + z^2} = \frac{1}{2}\frac{\sin\beta}{(1+\cos\beta)} \quad (15)$$

In order to solve the flow in the ξ plane we use our previous reasoning and first compute the volume flux F_ξ in the gap between ground and wing

$$F_\xi = \int_0^\eta U_\infty \left(\frac{\partial\phi}{\partial n}\right)_\xi d\eta$$

Substituting from Eq. (14)

$$F_\xi = \int_0^\beta U_\infty \left(\frac{\partial\phi}{\partial n}\right)_X d\beta$$

However, $(\partial\phi/\partial n)_X$ is the prescribed downwash in the X plane, given by Eq. (6)

$$F_\xi = \int_0^\beta w_0 \cos\beta d\beta$$
$$= w_0 \sin\beta$$

In order to write F_ξ as a function of η we would have to define an inverse function for β from Eq. (15). However, this is quite unnecessary for our purposes.

The gap width G_ξ is obtained from the following approximation:

$$G_\xi = \tfrac{1}{2} - [1/2(1+\epsilon)] \cong \epsilon/2$$

The vortex strength γ_ξ is the negative of the velocity in the gap

$$\gamma_\xi = -F_\xi/G_\xi = -(2w_0 \sin\beta/\epsilon)$$

This is integrated to get the lift distribution using Eq. (15);

$$\Gamma = \int \gamma_\xi \, d\eta = \frac{2w_0}{\epsilon}\int_{-\pi/2}^{\pi/2} \frac{\sin\beta d\beta}{2(1+\cos\beta)} \quad (16)$$
$$\Gamma = (w_0/\epsilon)\ln(1+\cos\beta)$$

Because Γ represents the potential discontinuity across the wing, and ϕ is the same for conformal points, Eq. (16) is valid in either plane.

We now calculate the vortex strength distribution using an entirely different approach which avoids the direct use of the conformal mapping. First, we know that a transforma-

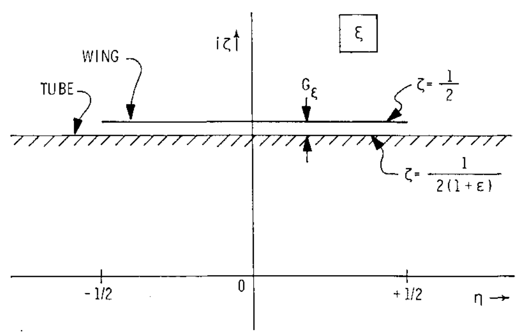

Fig. 8 The wing of Fig. 7 transformed to the ξ plane.

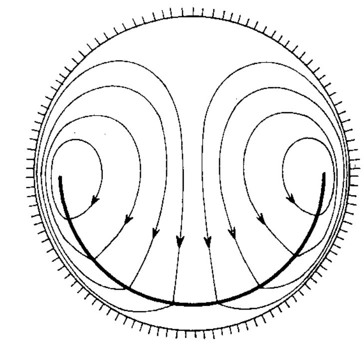

Fig. 9 Approximate streamline pattern in the vortex wake of the practical optimum wing configuration.

tion will preserve the angles that the streamlines make with any pair of conformal lines in the two planes. In particular, we know that in the ξ plane the streamlines above the wing are at right angles to the wing. The same must hold true in the X plane, so that for both planes the tangential velocity above the wing is zero. Furthermore, it is not even necessary to know the transformation explicitly; we can assume that whenever we have a lifting surface operating in close proximity to a solid boundary there exists some transformation which will give us Fig. 8, and therefore v_t is zero above the wing. With this knowledge we can dispense with the ξ plane and carry out the analysis directly from Fig. 7.

To a close approximation the gap is given by $G_X = \epsilon(1 + \cos\beta)$. We use the downwash condition from Eq. (7) to compute F_X, the volume flux in G_X;

$$F_X = \int_0^\beta v_n d\beta = w_0 \int_0^\beta \cos\beta d\beta$$
$$= w_0 \sin\beta$$
$$\gamma_X = -\frac{F_X}{G_X} = -\frac{w_0}{\epsilon}\frac{\sin\beta}{(1+\cos\beta)}$$

This is integrated as before;

$$\Gamma = \int_{-\pi/2}^{\pi/2} \gamma_x \, d\beta = \frac{w_0}{\epsilon}\ln(1+\cos\beta) \quad (17)$$

The agreement between Eqs. (16) and (17) shows that, as expected, this simpler and more intuitive method of analysis is quite valid.

Finally, application of Eq. (10) gives K

$$K = \frac{1}{\pi\epsilon}\int_{-\pi/2}^{\pi/2} \ln(1+\cos\beta)\cos\beta d\beta$$

The integral was calculated numerically giving the following result:

$$K = 0.37/\epsilon \quad (18)$$

The reader may be interested in knowing if any improvement on this value is obtained by taking the modified optimum configuration (Fig. 9), rather than the close approximation we have been using. The calculations for this are quite straightforward and yield two remarkably simple results,

$$\Gamma = w_0 \cos\beta/\epsilon, \text{ and } K = 1/2\epsilon \quad (19)$$

Not only does Eq. (19) represent a slight improvement over the value given by Eq. (18), but if we compare to Eq. (12), we see that the wing in the tube has only 43% of the induced drag of the planar wing in ground effect, both wings having the same lift, span, and minimum clearance; therefore, from a strict induced drag standpoint, enclosure within a tube has yielded a substantial benefit.

It is somewhat interesting to go further and compute the power requirements implied by Eq. (19). To do this we return to dimensional units, letting ϵ^* = dimensional clearance. Then $\epsilon = 2\epsilon^*/b$. This is substituted into Eq. (19), which is used in Eq. (9) to get the induced drag coefficient. The

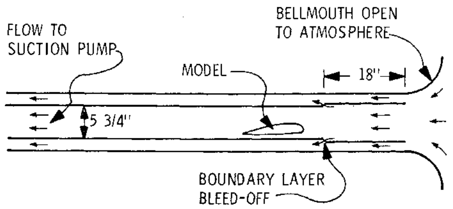

Fig. 10 Apparatus used to test vehicle models.

power P necessary to produce the lift can be computed from this. We obtain

$$P = (8/\pi)\epsilon^* W^2/\rho U_\infty b^3 \tag{20}$$

where W = vehicle weight.

Equation (20) demonstrates the seldom appreciated fact that the power required for lift is quite independent of the streamwise length of the lifting surface and is inversely proportional to velocity. This is true even for a wing in a freestream. For a ram wing in a tube we may further note that the induced power requirement is directly proportional to the minimum clearance.

It is, of course, quite obvious that Eq. (17) only tells us the theoretical lift distribution for minimum induced drag. We have no clue as to how to go about actually producing this distribution. This could theoretically be done in an infinite number of ways; the actual shape for optimum over-all performance, however, must take into account pitching moment and boundary-layer effects, which will greatly narrow the field of choice. We can only say at this point that the trailing edge should be a semicircle. From aeronautical intuition we might conclude that the lift distribution will tend toward the optimum for any reasonable streamlined shape, as it does for wings in a freestream. For vehicle design such as shown in Fig. 1 this is especially true because of the very low aspect ratio.

The results obtained so far are based on linear theory and are only valid for very thin vehicles which produce small disturbance velocities. It may be valid to assume that the disturbances due to lift effects will indeed be quite small, since the estimated lift coefficients for high-speed tube vehicles are on the order of 0.3. However, there will be a substantial change in the x velocity due to the thickness of the vehicle. Assuming the cross-sectional area of the vehicle is roughly constant, we can define a blockage ratio $r \equiv A_v/A_t$. Using one-dimensional incompressible mass continuity we obtain the x velocity past the vehicle $U/U_\infty = 1/(1 - r)$.

As a crude method to account for this blockage effect we can substitute U for U_∞ in Eq. (5). This results in modifying

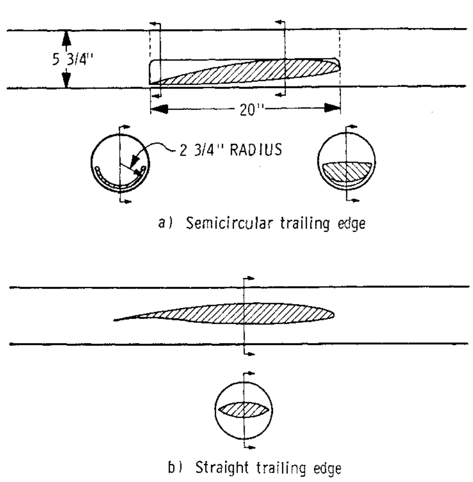

Fig. 11 Typical models used in the experiments.

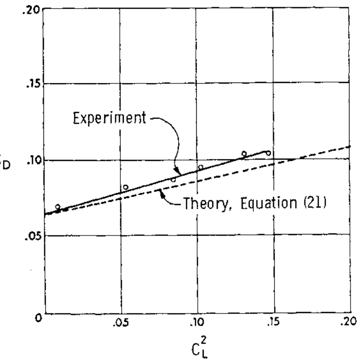

Fig. 12 Experimental results for a model as shown in Fig. 11a, with a clearance of $^5/_{16}$ in.

Eqs. (19) and (20) into the following forms:

$$K = [1/2(1 - r)\epsilon] \tag{21}$$

$$P = [8(1 - r)\epsilon^* W^2/\pi\rho U_\infty b^3] \tag{22}$$

Equation (22) tells us that the power required for lift is decreased by high blockage ratios. There is, of course, the opposite effect on the parasite drag.

When the vehicle design incorporates an axisymmetric body supported by a number of short ram wing pads, as in Ref. 3, there is some difficulty in deciding the most advantageous location of these pads. If they are located in front of and behind the body they will suffer less parasite drag, but the favorable effects of blockage will be lost; that is, the power required is given by Eq. (20) rather than Eq. (22). However, if they are located under the vehicle (which is simpler structurally) they will create high parasite drag and may actually cause the flow in the region between the pad and the vehicle to be choked below the design velocity of the vehicle. When the entire vehicle is a ram wing, however, the difficulties are avoided and the advantages shown by Eq. (22) can be utilized.

Comparison with Experiments

Several experimental tests on tube vehicle models were performed using a setup such as shown in Fig. 10.[11] Tests

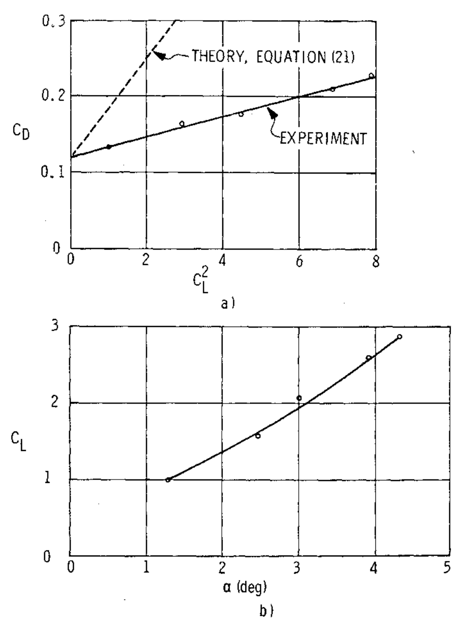

Fig. 13 Typical experimental results for a model as in Fig. 11a, with a clearance of $^1/_8$ in. ($\epsilon = 0.045$), showing the effect of viscosity in reducing the induced drag.

were run on models with semicircular trailing edges and with straight trailing edges, as in Fig. 11.

The experiments showed reasonable agreement with the theory as long as ϵ was not too small, but for very small clearance the effects of viscosity become important. Typical results are shown in Figs. 12 and 13, these are for two models with semicircular trailing edges. Figure 12 shows the results for a model of $5\frac{1}{8}$ in. width, 20 in. chord, and 30% blockage, which gives a predicted K of 5.8 using Eq. (21). (The inside diameter of the tube was $5\frac{3}{4}$ in.). The experimentally determined K was 4.9, which is within the expected accuracy. Note that in this case the clearance between the model and the tube is $\frac{5}{16}$ in. The Reynolds number for this test was 4.6×10^5.

Figure 13 gives the results for a model of $5\frac{1}{2}$ in. width and 35% blockage, and similar in all other respects to the first model. The clearance in this case is $\frac{1}{8}$ in., giving a predicted K of 18. However, this prediction does not allow for viscous effects, which are quite dramatic at this small clearance. Note the change between Figs. 12 and 13 in the magnitudes of the lift coefficient; the second model attained the remarkably high C_L of 4.3. The experimentally determined K was 66. Even though this shows rather poor agreement with the theory, it was felt that including these results was quite important, for two reasons. First, it is interesting that viscosity tends to increase the efficiency of the wing, as measured in terms of lift-drag ratio. Second, the results point up one defect of the experiment, as explained below.

In the experimental situation the model and tube were stationary and the air was moving, so that a boundary-layer developed in the thin gap between the model and the tube. Although great care was taken to insure that the flow was uniform upon entering a test section and the boundary-layer effect would be minimized, it appears that this test situation is simply not an adequate simulation of the real situation in which the vehicle is moving and the air and tube are stationary. The boundary layer has the effect of reducing the effective clearance ratio ϵ of Eq. (21), so that the model had much lower induced drag than anticipated. (The parasite drag, of course, is increased by this effect.)

We can expect that in the real situation with the vehicle moving we will obtain better agreement. Also, with full scale vehicles and clearances on the order of one foot (as opposed to $\frac{1}{8}$ in.), the boundary layer on the vehicle will have a much smaller relative thickness, so that our theoretical analysis should become even more accurate.

Figure 13b is included to show the very high lift curve slopes which can be achieved; these are up to 80 times the value which would be obtained in freestream using slender body theory.

The experiments very definitely did confirm that the semicircular wing was superior to the flat wing, and that induced drag is proportional to the square of the lift. Also, the minimum clearance is certainly the crucial parameter in determining power losses, although the simple relationship given by Eqs. (21) and (22) was not always valid in the test situation.

Conclusion

The problem of finding the minimum induced drag of a ram wing can be greatly simplified if the clearance ratio ϵ is very small. The power required to support a given vehicle weight will be proportional to ϵ, and for the case of a ram wing in a tube this power is reduced for vehicles of large blockage as shown by Eqs. (22). With very small clearances viscous effects come into play and act to reduce the already small induced drag even further, to the point where it is only a small fraction of the total drag. Certainly, the ram wing concept looks very promising as a method of supporting vehicles in tubes; probably the major problems remaining with such vehicles are finding methods of reducing the parasite drag and determining efficient means of propulsion.

References

[1] Strand, T., Royce, W., and Fujita, T., "Performance Theory for High Speed Ground Effect Machines," Rept. 11, 1961, Vehicle Research Corp.

[2] Yaffee, M. L., "Ram Wing Studied as Transit Vehicle," *Aviation Week and Space Technology*, Jan. 2, 1967.

[3] "Project Tubeflight," PB 174085, Sept. 1966, Rensselaer Polytechnic Institute.

[4] Munk, M., "The Minimum Induced Drag of Aerofoils," Rept. 121, 1921, NACA.

[5] Cone, C. D., "The Theory of Induced Lift and Minimum Induced Drag of Nonplanar Lifting Systems," TR R-139, 1962, NASA.

[6] Cone, C. D., "The Aerodynamic Design of Wings with Cambered Span Having Minimum Induced Drag," TR R-152, 1963, NASA.

[7] Glauert, H., "The Interference on Characteristics of an Aerofoil in a Wind Tunnel of Circular Cross Section," R. & M. 1453, Dec. 1931, Great Britain Aeronautical Research Council.

[8] Millikan, C. B., "Lift Distribution on a Wing in a Circular Tunnel," *Transactions of the ASME*, Vol. 54, No. 8, 1932.

[9] Landahl, M. T. and Ashley, H., *The Aerodynamics of Wings and Bodies*, Addison-Wesley, Reading, Mass., 1965.

[10] Milne-Thomson, L. M., *Theoretical Hydrodynamics*, MacMillan, New York, 1960.

[11] de Haller, P., "La Portance et la Trainee Induite Minimum d'une Aile au Voisinage du Sol," *Mitteilunger Aus Dem Institut Für Aerodynamik Der Technische Hochscule*, Zurich, No. 5, 1936.

[12] Wieselsberger, C., "Wing Resistance Near the Ground," TM 77, 1922, NACA.

[13] Carter, A. W., "Effect of Ground Proximity on the Aerodynamic Characteristics of Aspect-Ratio-1 Airfoils With and Without End Plates," TN D-970, 1961, NASA.

[14] Fink, M. P. and Lastinger, J. L., "Aerodynamic Characteristics of Low-Aspect-Ratio Wings in Close Proximity to the Ground," TN D-926, 1961, NASA.

[15] Lockheed, "Wind Tunnel Investigations of Single and Tandem Low-Aspect-Ratio Wings," Rept. 16906, March 1964, TRECOM TR 63-63, U.S. Army Transportation Research Command.

[16] Barrows, T. M., "Optimum Lift-Drag Ratio for a Ram Wing Tube Vehicle," M.S. thesis, June 1968, Massachusetts Institute of Technology.